NUMERICAL PLASTICITY AND CREEP ANALYSIS BASED ON THE FRACTION MODEL AND EXPERIMENTAL VERIFICATION FOR AISI 304

P. MEIJERS, G.T.M. JANSSEN
Institute TNO for Mechanical Constructions, Delft, The Netherlands

J. BOOIJ
Laboratory of Applied Mechanics, Delft University of Technology, Delft, The Netherlands

SUMMARY

The main problem related to plasticity analysis with strainhardening and to a still greater extent to creep analysis is the fact that there is no phenomenological description available that has been sufficiently verified by experiments. This is true even for general uni-axial loading histories although for such situations far more experimental data are available than for multi-axial loading. For an efficient operation of fast breeders the temperature level is such that creep deformation has to be taken into account, whereas time-independent plastic deformations, due mainly to thermal loading during emergency conditions, cannot be avoided. This makes an accurate description of these non-linear deformations indispensable.

A finite element description of creep and plastic deformations based on the fraction model of BESSELING has been developed and applied to components of nuclear reactors. This model was chosen because it was expected to give the best results. In this description for time-independent plastic deformations a volume element is thought to be subdivided into a set of parallel fractions of elastic-ideally plastic material with different yield limits. When necessary a small amount of isotropic hardening for each fraction may be included. The required material parameters are obtained from a uni-axial tension or a torsion test. In case of creep the parallel volume fractions show only secondary creep but with different creep rates. Due to the interaction of the fractions primary creep and recovery may be explained qualitatively.

To determine the accuracy of the phenomenological description for plastic deformations in components of AISI 304, a set of bi-axial experiments on thin-walled tubes has been carried out at room temperature, with loading programmes that are a combination of tension, torsion and internal pressure. They cover the whole range of bi-axial states of stress.

A remarkable result was the significant time effect at room temperature and at very low strain rates. This required a modification of the constitutive equations and lead to a description of the interaction of creep and plasticity which may also be applicable at high temperatures.

The experimental set-up is shown and the experimentally obtained stress-strain histories are compared with the theoretical results predicted with the fraction model and other theories.

Some results of an experimental programme for verification of the description of creep under general uni-axial and bi-axial loading programmes are shown as well.

1. Introduction

The main problem related to creep analysis and to the description of plastic deformations for materials showing strain-hardening is the fact that there are no constitutive equations available that have been sufficiently verified with the aid of experiments. This is even true for general uni-axial loading histories, although far more experimental data are then available than for bi-axial or tri-axial loading programmes.

The development of the high-speed computers and numerical methods adapted to these computers have made it possible to perform an elastic-plastic or creep analysis for structures with a complex geometry which is absolutely impossible with analytical methods. However, such an effort is only justified when a reliable result can be obtained. That is a reason why much attention is focused on the constitutive equations. Another important stimulus for this research has come from the nuclear reactor projects, specially the sodium-cooled fast breeders. It is well known that for an efficient operation of fast breeders the temperature level is such that the creep deformation has to be taken into account, whereas also time independent plastic deformations due mainly to thermal loading during emergency conditions must be evaluated.

The creep and plasticity research to be discussed was started by developing a finite element description and a corresponding computer code, based on the so-called fraction model of BESSELING described using continuum theory in [1]. This description was chosen because it was expected to give more accurate results than other constitutive equations available and generally applied. A finite element description for time independent plastic deformations based on this model is discussed in [2,3] and a similar description for creep in [4].

Although the fraction model can qualitatively describe certain phenomena of plastic deformation and creep better than other current models, and the finite element programmes based on this description were applied to components of SNR 300, it was still an open question as to how accurate this description was for nuclear reactor materials. Especially for creep very few experiments have been carried out for verification of the description by the fraction model. The only comparison known to the authors has been made by LAMBERMONT and BESSELING for a Mg-alloy [5].

This is the reason why for stainless steel WN 1.4948 (AISI 304) an experimental programme has been started; it should determine the accuracy of this description for a set of bi-axial loading histories chosen such that the results may give reliable predictions for general multi-axial loading histories.

Uniform, bi-axial states of stress which cover the whole range of principal stress ratios can be obtained when thin-walled cylinders are loaded by combinations of tension, torsion and radial pressure. The discussion on the experimental verification will in the present paper be concentrated on the plastic deformation of WN 1.4948 at ambient temperature. Since this material showed considerable time effects even at 20 °C and at very low strain rates, it was necessary to combine the description for creep and time independent plastic deformations. An experimental programme was also initiated for verification of the creep description at high temperature starting with very accurate uni-axial and then also bi-axial tests on thin-walled tubes.

Having reached a sufficiently reliable description, the question arises whether a

certain multi-axial deformation history is allowable from the point of low cycle fatigue and creep rupture. Therefore experiments have been started for the same material to collect data on the effect of bi-axiality on low-cycle fatigue. Again these experiments are being carried out on thin-walled tubes loaded by combinations of cyclic axial load, torsion and radial pressure.

2. Analysis

2.1 Plastic deformation with strainhardening

In the discrete description of the continuum theory of plasticity developed in [1] a finite element is thought to be subdivided into a number of parallel subelements with an elastic-ideally plastic behaviour or showing some isotropic hardening, but with different yield limits. The vector of generalized plastic strain components of subelement k in element j is denoted $\bar{\varepsilon}^{jk}$, the vector of generalized thermal strains $\varepsilon^{\theta j}$ and the vector of total strains is ε^{j}. The yield surface in the space of generalized elastic strain components

$$\varepsilon^{ejk} = \varepsilon^{j} - \varepsilon^{\theta j} - \bar{\varepsilon}^{jk} \tag{1}$$

is indicated;

$$\phi^{jk} - \frac{1}{6}\frac{(\sigma_y^k)^2}{G} = 0 \tag{2}$$

where σ_y^k is the yield stress in uni-axial tension of subelement k, and G the shear modulus. When the VON MISES yield criterion is accepted, ϕ^{jk} is the specific distortional elastic energy, which is in terms of the elastic strains,

$$\phi^{jk} = \frac{\frac{1}{2}\,\varepsilon^{Tejk}\, S_D^j\, \varepsilon^{ejk}}{Y^j} \tag{3}$$

The fact that the vector of plastic strain increments $\Delta\bar{\varepsilon}^{jk}$ is normal to the yield surface in generalized stress space [6] may be written as:

$$S^j\, \Delta\bar{\varepsilon}^{jk} = \lambda \frac{\partial \phi^{jk}}{\partial \varepsilon^{ejk}} \tag{4}$$

where S^j is the stiffness matrix of element j. Elimination of λ from (2) and (4) yields for the strain increments:

$$\Delta\bar{\varepsilon}^{jk} = Y^{jk}\left[\Delta\varepsilon^{j} - \Delta\varepsilon^{\theta j}\right] \qquad \text{if} \qquad \phi = \frac{1}{6}\frac{(\sigma_y^k)^2}{G} \tag{5}$$

and

$$\Delta\bar{\varepsilon}^{jk} = 0 \qquad \text{if} \qquad \phi < \frac{1}{6}\frac{(\sigma_y^k)^2}{G}\,. \tag{6}$$

The general expression for the yield matrix is:

$$Y^{jk} = [S^j]^{-1} \frac{\left[\frac{\partial \phi^{jk}}{\partial \varepsilon^{ejk}}\right]\left[\frac{\partial \phi^{jk}}{\partial \varepsilon^{ejk}}\right]^T}{\left[\frac{\partial \phi^{jk}}{\partial \varepsilon^{ejk}}\right]^T [S^j]^{-1} \left[\frac{\partial \phi^{jk}}{\partial \varepsilon^{ejk}}\right]} \tag{7}$$

and for the VON MISES yield surface

$$Y^{jk} = \frac{[S^j]^{-1}\, S_D^j\, \varepsilon^{ejk} \varepsilon^{Tejk}\, S_D^j}{\varepsilon^{Tejk}\, S_D^j\, [S^j]^{-1} S_D^j\, \varepsilon^{ejk}}\,. \tag{8}$$

The variation of the potential energy for kinematically admissible variations of the displacements - where the non-elastic strains are treated as fixed quantities - is zero for an equilibrium position. This provides us with a set of linear equations for the increment of the displacement vector in terms of the increments of the mechanical and possibly thermal loading. The matrices relating the vector of element strains to the structural displacement vector u, the vector of prescribed displacements u^o and temperature vector θ^o, are defined by the relations:

$$\varepsilon^j = D^j u^j = D^j \left| \tilde{L}_1^j \; L_2^j \right| \begin{vmatrix} u \\ u^o \end{vmatrix} \quad , \quad \varepsilon^{\theta j} = D_3^j \, \theta^j = D_3^j \, L_3^j \, \theta^o . \tag{9}$$

The equations for displacement increments are:

$$[S_1 - Y_1]\Delta u = \Delta f^o - [S_2 - Y_2]\Delta u^o + [S_3 - Y_3]\Delta\theta^o \tag{10}$$

where f^o is the external load vector and:

$$S_i = \sum_{j=1}^{\ell} L^{Tj} \, D^{Tj} \, S^j \, D_i^j \, L_i^j \; ; \; Y_i = \sum_{j=1}^{\ell} \sum_{k=1}^{n_j} \psi^k \, L^{Tj} \, D^{Tj} \, S^j \, Y^{jk} \, D_i^j \, L_i^j \; (i=1,2,3) \tag{11}$$

$$(D_1^j = D_2^j = D^j)$$

Integer n_j indicates the number of plastic subelements in element j.

Having obtained the increment of the displacement vector we can derive the generalized elastic strain vectors of each element. The stress vector, $\tilde{\sigma}$, for an arbitrary point in an element j is in terms of the increments of the vector of generalized elastic strains:

$$\Delta\tilde{\sigma} = G^j \, \Delta\tilde{\varepsilon} = G^j \, C^j \, \Delta \left[\varepsilon^j - \varepsilon^{\theta j} - \sum_k \psi^k \, \bar{\varepsilon}^{jk} \right] \tag{12}$$

where matrix C^j relates the generalized strain vector to the vector of local strain components $\tilde{\varepsilon}$.

The required constants, viz. the volume fractions ψ^k and the yield limits, can be directly determined from a uni-axial tension or a torsion test. The tension curve is approximated by a piecewise linear curve, see Fig. 1. For this example, three elastic-ideally plastic fractions have been chosen. In point 1, the first volume fraction starts yielding and at point 3 the third and last fraction reaches the yield limit of that volume fraction. The yield limits follow directly from the strains at points 1 till 3:

$$\sigma_y^k = E \, \varepsilon_x^k \qquad (k=1,2,3) \tag{13}$$

The volume fractions are determined by the tangents of the line segments since:

$$\Delta\sigma_x = E \left[1 - \sum_{k=1}^{n_1} \psi^k \right] \Delta\varepsilon_x \quad , \tag{14}$$

and the condition:

$$\sum_k \psi^k = 1 \quad , \tag{15}$$

n_1 being the number of plastic subelements at stress level σ_x. It is also possible to include in the description a small amount of isotropic strain-hardening.

A computer programme based on this formulation has been developed for axi-symmetric and plane two-dimensional structures and applied to components of the SNR 300 project

loaded under thermal and mechanical loading. Fig. 2 shows an example of the elastic-plastic analysis of the bellows in a compensator loaded by prescribed axial displacements and an internal pressure [7]. In the analysis it is assumed that the fictitious finite subelements as a whole either yield or remain elastic; this implies that the transition between the elastic and the plastic region is along the element boundaries. The approximate uniaxial stress-strain curve valid for the material at the operating temperature is the curve shown in Fig. 1.

2.2 Creep analysis

In the discrete description of creep [4] based on the continuum theory developed in [1], a finite element j is again assumed to be subdivided into a number of parallel subelements. All these subelements show only secondary creep, but with different creep rates. Due to the interaction of these volume fractions, primary creep and after effects may be described as well.

Vector $\bar{\varepsilon}^{jk}$ is now the vector of generalized creep strains for subelement k in element j. For this subelement the rate of energy dissipation per unit volume, which is assumed to be a function of the elastic strains and temperature, is indicated g^{jk}. Hence:

$$\varepsilon^{Tejk}\, S^j\, \frac{d\bar{\varepsilon}^{jk}}{dt} = V^j\, g^{jk}(\varepsilon^{ejk}, \theta^j) \qquad (16)$$

The assumption that $d\bar{\varepsilon}^{jk}/dt$ is normal to the surface of constant rate of dissipation [8] in stress space yields the relation:

$$S^j\, \frac{d\bar{\varepsilon}^{jk}}{dt} = \mu V^j\, \frac{\partial g^{jk}}{\partial \varepsilon^{ejk}} \quad . \qquad (17)$$

Elimination of μ from eq. (17) with help of eq. (16) leads to the following expression for the dissipation vector of subelement k in element j:

$$\frac{d\bar{\varepsilon}^{jk}}{dt} = V^j \left[\varepsilon^{Tejk}\, \frac{\partial g^{jk}}{\partial \varepsilon^{ejk}}\right]^{-1} g^{jk} \left[S^j\right]^{-1} \frac{\partial g^{jk}}{\partial \varepsilon^{ejk}} \quad . \qquad (18)$$

It is known from experiments that a hydrostatic state of stress does not influence the creep of metals, and hence the dissipation function in an arbitrary point of volume fraction k is a function of the distortional elastic energy and the temperature. In the discrete description we assume it to be a function of the specific distortional energy averaged over the subelement concerned and the average temperature over the element.

The following expression for g^{jk} has been assumed in the calculations:

$$g^{jk} = \gamma(\theta^j) \left[\frac{\frac{1}{2}\, \varepsilon^{Tejk}\, S_D^j\, \varepsilon^{ejk}}{(p^k)^2\, V^j}\right]^n \qquad (19)$$

The difference in strain for the subelements is determined by factor p^k. The number n is assumed to be equal for all elements. An analysis can also be carried out with more general expressions of the distortional elastic energy, but for the time being there are no sufficiently accurate experimental data available to justify a more refined description.

As to the temperature dependance, it is well known from theoretical considerations that it is an exponential function of the absolute temperature. The simplest expression, which will be applied here, is:

$$\gamma(\theta) = \gamma_o \, e^{-\frac{T_o}{T}} \tag{20}$$

where T is the absolute temperature and T_o the activation energy divided by the gas constant.

With eq. (19) the creep rate is:

$$\frac{d\bar{\varepsilon}^{jk}}{dt} = \frac{\gamma(\theta^j)}{(p^k)^2} \left[\frac{\frac{1}{2} \varepsilon^{Tejk} S_D^j \varepsilon^{ejk}}{(p^k)^2 V^j} \right]^{n-1} [S^j]^{-1} S_D^j \varepsilon^{ejk} = c^{jk} \tag{21}$$

Application of the principle of minimum potential energy leads to the set of first-order differential equations for the components of the unknown displacement vector u:

$$\sum_j L^{Tj} D^{Tj} S^j D^j L^j \frac{du}{dt} = - \sum_j L^{Tj} D^{Tj} S^j \left[D^j L^{jo} \frac{du^o}{dt} - \frac{d\varepsilon^{\theta j}}{dt} - c^j \right] + \frac{df^o}{dt} \tag{22}$$

where

$$c^j = \Sigma \psi^k \, c^{jk} \tag{23}$$

When, for the time being, it is assumed that the required creep constants are available, simultaneous numerical integration of eq. (21) and eq. (22) with more or less advanced methods gives us the displacement vector u(t).

Superposition of the contributions of the subelements gives the stresses in an arbitrary point of the element. The formal expression is identical to (12).

It is more difficult to obtain the creep parameters ψ^k and p^k, from a uni-axial creep on relaxation test than the corresponding parameters for time independent plastic deformations. Moreover, there is often an enormous scatter in the available data. This is mainly due to the exponential effect of temperature and the highly non-linear dependance of the creep strain rate on the stress level, which implies that to determine the creep parameters as a function of stress and temperature it must be possible to control with extreme accuracy the temperature and load of the specimen.

Having available a number of uni-axial creep curves, we can obtain the best approximation for stationary creep parameters n and $F(\theta)$ in the degenerate expression of eq. (21):

$$\dot{\bar{\varepsilon}} = F(\theta) \, \sigma^{2n-1} \tag{24}$$

In order to reach the stationary creep rate it is necessary that the following relation holds between the volume fractions and the creep parameters of these volume fractions [5]:

$$\sum_k \psi^k \left(\frac{F}{F^k} \right)^{\frac{1}{2n-1}} = 1 \tag{25}$$

In addition, a set of non-linear, ill-conditioned equations for constants ψ^k and F^k can be derived. Another procedure is that a very restricted number of volume fractions is chosen and starting from an assumed combination, the parameters are modified in a systematic way until a sufficiently accurate approximation of the experimental creep and/or relaxation curve is obtained. Fig 3 shows theoretical curves for various parameter combinations and the same secondary creep rate. The figure illustrates that in this case it is fairly simple to obtain an approximation of the experimental creep curve. The relation between the parameters p^k and F^k follows from eq. (19).

A computer programme based on this description is available for axi-symmetric struc-

tures [4]; it has been applied for details of nuclear reactor components. The computation cost is only slightly increased with respect to that of a creep analysis, taking into account only secondary creep.

2.3 Description of combined creep- and plastic deformations

A combination of the models discussed in the preceding paragraphs, the uni-axial case of which is shown in Fig 4-a, makes it possible to give a description of the interaction of creep and time-independent plastic deformations. The incremental equations can be derived in a similar way as discussed in the preceding paragraphs. The general equation corresponding to eq. (10) and eq. (22) is:

$$[S_1-Y_1]\Delta u = \Delta f^o - [S_2-Y_2]\Delta u^o + [S_3-Y_3]\Delta\theta^o + \sum_j L^{Tj} D^{Tj} S^j c^j \Delta t \qquad (26)$$

where in the yield matrices the summation is extended over the plastic subelements whereas in the creepvector, the summation is restricted to the creep fractions.

First it was planned to determine the accuracy of the creep and time-independent plasticity description for the material WN 1.4948 (AISI 304) separately at ambient temperature and later coupled for temperatures of 550-600 °C. However, the significant time-effect at room temperature and at very low strain-rates as mentioned above made it necessary to include creep effects from the beginning [9]. These effects are not dominant at 20 °C and therefore only a single creep fraction (Fig 4-a) was chosen, which implies that only secondary creep can be described.

The discussion on the determination of the model parameters for the combination of creep and plastic deformations will be restricted here to the behaviour of WN 1.4948 at ambient temperature and the creep effects collected in a single subelement.

Fig. 5 shows stress-strain curves for three different strain-rates and an approximation for the "static" stress-strain curve ($\dot{\varepsilon}=0$). An approximation of this curve can also be obtained by allowing for relaxation periods during a tension test. The total load per unit area of the cross-section may be split as follows (Fig 5):

$$\sigma_x = \sigma_s(\varepsilon_x, T) + \sigma_c(\dot{\varepsilon}_x, \varepsilon_x, T) \qquad (27)$$

For sufficiently large values of ε_x the creep contribution σ_c tends to be independent of the total deformation, and the creep parameters have been determined from this stationary situation, where $\sigma_c = \sigma_{co}$. Assuming a volume fraction ψ^1, one can obtain an approximation for the creep constants F^1 and n from equation:

$$\dot{\varepsilon}_c = F^1 \left(\frac{\sigma_{co}}{\psi^1 \sigma_y^1}\right)^{2n-1} \qquad (28)$$

when curves for different strain rates are available. The constant σ_y^1 has only been introduced for scaling. An approximation of the creep fraction may be obtained from the response to a step load. This resulted in a rather large creep fraction, which implies a strong reduction in the slope of the stress-strain curve at very low strain rates in the elastic range. This was not confirmed by the experiments. A volume fraction $\psi^1 = 0.15$ was chosen as a compromise.

In case there is a small amount of isotropic hardening in plastic deformation this can be taken into account by a small parameter h^k defined such that (see eq. (5)):

$$\Delta \bar{\varepsilon}^{jk} = (1-h^k)\, Y^{jk} \left[\Delta\varepsilon^j - \Delta\varepsilon^{\theta j}\right] . \qquad (29)$$

When consistently yield matrix Y^{jk} is replaced by:

$$\bar{Y}^{jk} = (1 - h^k) Y^{jk} \qquad (30)$$

and there is in addition a creep fraction ψ^1, eq. (14) for the tangents of the line segments of the "static" stress-strain curve becomes:

$$\Delta\sigma_x = E \left[1 - \psi^1 - \sum_{k=2}^{n_1} (1 - h^k)\psi^k\right] \Delta\varepsilon_x . \qquad (31)$$

The parameters h^k are assumed to be equal for all subelements. Under this condition the slope of the line segments and eq. (15) provide us with a sufficient set of relations to determine $\psi^k (k \geq 2)$ and h.

3. Bi-axial plasticity experiments for WN 1.4948

3.1 Test apparatus and specimens

Fig 6 shows the geometry of the tubular specimen. The manufacturing has been carried out very carefully, so as to keep the residual stresses as low as possible.

The test set-up is indicated in Fig 7. A torsion testing machine has been modified to carry out tension, compression and internal pressure tests as well. The axial load and the twisting moment are measured by a load cell, and the internal pressure by an electronic pressure gauge. To measure the axial strain, special extensometers have been designed; for the angle of twist, a precise potentiometer was made. The tangential strain is measured with four high-strain strain-gauges on the outside of the tube.

The measured signals are amplified and recorded on x-y and x-t recorders. At the same time the signals are scanned and stored on tape. In a computer the experimental data are converted into stresses and strains, and fed into a plotter. For a more detailed discussion we refer to [10].

3.2 Comparison of experimental results and theoretical predictions

A set of model parameters has been based on tension curves for different strain rates and, also, on a torsion test with relaxation periods. Table I shows the numerical results. Subsequently, approximately 30 experiments have been carried out to consider the accuracy of the description for bi-axial loading histories. All these loading programmes are combinations of a uniform axial stress and torsion or combinations of axial load and internal pressure. With these combinations it is possible to cover the whole range of principal stresses $-1 \leq \sigma_1/\sigma_2 \leq 1$. Load reversals and rotation of the principal stresses during the loading programmes were included since the theoretical prediction of the deformations under such circumstances is very sensitive for the constitutive equations applied.

A comparison of theoretical and experimental results, where the theoretical results are based on parameters of a tension and torsion test are shown in Figs 8 - 13 for 6 typical loading histories. The input for a theoretical analysis was the measured strain history as a function of time.

The results are quite encouraging, although the description of the creep effect is not very accurate. This is clearly illustrated in Figs 8 and 9 at points where in the experimental curve the load is sharply increased. In cyclic loading, the elastic range is consistently smaller than expected from theory; most pronounced is this effect in Fig. 13. The

experiments also confirmed the expectation that the isotropic hardening parameter h reduces with an increase of the plastic strains. Therefore a refinement of the description to take into account the diminishing of the isotropic hardening with the accumulated plastic strain would also be useful.

During the plastic deformation in Fig 12 the stress ratio σ_1/σ_2 increases from 0.5 to 1 and near the point where $\sigma_1/\sigma_2 = 1$ the normal to the yield surface in stress space, which indicates the direction of the plastic strain vector, strongly rotates for the VON MISES yield surface. Under such circumstances relatively more pronounced differences between description and experiment can be expected.

The experimental results may be used to verify any description currently used or in the stage of development. Fig 4-b shows a possible adaptation of the model under investigation. The description becomes more complicated and contains more model parameters. A preference for this description comes from the fact that there is no creep deformation in the elastic range, which is confirmed by the low temperature experiments. On the other hand, the simpler model of Fig 4-a is in principle applicable for the description of the combination of creep and time-independent plastic deformations at elevated temperature. In that case creep becomes more dominant and therefore more than one creep fraction is required to take into account primary creep as well. A continuation of the experimental verification in this direction is going on.

Acknowledgement

The authors are very grateful to the Project Group of Nuclear Energy TNO, for the financial support and the coordination of this project in the frame of a support programme for the Dutch industry (Neratoom). The authors are also grateful to prof.dr.ir. J.F. Besseling for his valuable advice and to all other collaborators of this project.

Table I. Model parameters from tension and torsion test.

k	tension test		torsion test	
	ψ^k	σ_y^k [N/mm^2]	ψ^k	σ_y^k [N/mm^2]
1	0.1500	100.0	0.1500	100.0
2	0.4493	114.6	0.6483	129.2
3	0.2819	152.8	0.1241	258.5
4	0.0556	267.4	0.0559	439.4
5	0.0348	477.5	0.0143	775.4
6	0.0200	764.0	0.0047	1292.0
7	0.0084	1528.0	0.0027	2585.0
$F^1=0.5024.10^{-6}$ [s^{-1}] n = 2.5		$\sigma_{co}=36$ [N/mm^2] h = 0.0164	$F^1=0.9721.10^{-6}$ [s^{-1}] n = 2.5	$\tau_{co}=17$ [N/mm^2] h = 0.011
$E = 1.91.10^5$ [N/mm^2]			$\nu = 0.28$	

References

[1] BESSELING, J.F.,"A theory of elastic plastic and creep deformations of an initially isotropic material showing anisotropic strain-hardening creep recovery and secondary creep." J. Appl. Mech., 25, 529-536 (1958).

[2] MEIJERS, P."Elastic-plastic deformation of thick-walled cylinders." Proc. First Int. Conf. Pressure Vessel Technology, Delft, 1969, Part I. Design and Analysis, 19-34.

[3] ZIENKIEWICZ, O.C., NAYAK, G.C. and OWEN, D.R.J. "Composite and 'overlay' models in numerical analysis of elasto-plastic continua". Int. Symp. on Foundations of Plasticity, Warsaw, 1972.

[4] MEIJERS, P., "A discrete description of creep in axi-symmetric structures, taking into account primary creep and recovery." Inst. TNO for Mechanical Constructions, Rep. no 10019, 1973.

[5] LAMBERMONT, J.H. and BESSELING, J.F., "An experimental and theoretical investigation of creep under uni-axial stress of Mg-alloy." Proc. IUTAM Symposium Creep in Structures, Gothenburg, 1970, 39-63.

[6] DRUCKER, D.C."A more fundamental approach to plastic stress-strain relations." Proc. First USA National Congr. Appl. Mech. 1951, 487-491.

[7] GEERTSEMA, H. "Elastic-plastic analysis of the bellows in the compensator of the SNR steam generator." Rep. No. 10018/2, 1973.

[8] ZIEGLER, H. "Zwei Extremalprinzipien der irreversiblen Thermodynamik." Ingenieur Archiv. 30, 410-416, (1961).

[9] JANSSEN, G.T.M. and MEIJERS, P. "Bi-axial plasticity experiments with respect to AISI 304-L." Inst. TNO for Mechanical Constructions. Rep. no. 10664/1, 1974.

[10] BOOY, J. and WERFF., K. v.d. "Plasticity experiments on austenitic strainless steel tubes." Dept. Mechanical Engineering, Delft University.

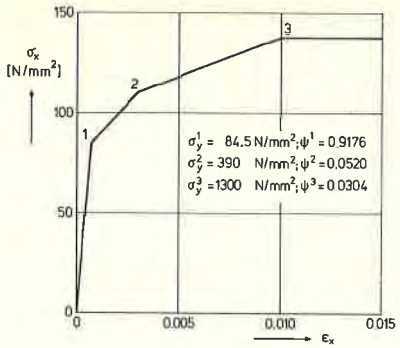

Fig 1. Approximate stress-strain curve.

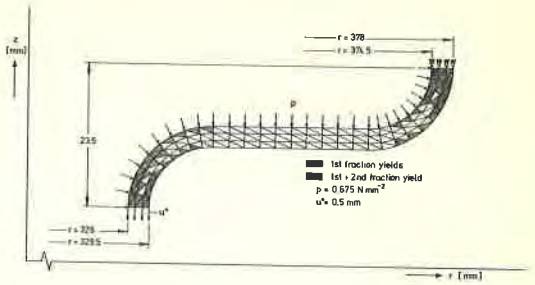

Fig 2. Elastic-plastic analysis of bellows.

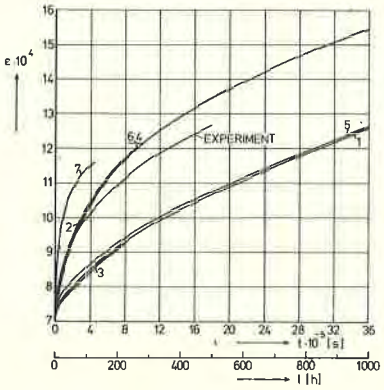

№	ψ_1	ψ_2	ψ_3	$\frac{F_1}{F}$	$\frac{F_2}{F}$	$\frac{F_3}{F}$
1	0.2	0.6	0.2	0.010	2.318	100
2	0.2	0.6	0.2	0.001	7.991	1000
3	0.1	0.8	0.1	0.001	2.063	1000
4	0.2	0.6	0.2	0.001	13.532	100
5	0.2	0.5	0.3	0.010	1.278	100
6	0.2	0.5	0.3	0.001	9.516	100
7	0.333	0.333	0.333	0.003	40.187	2000

Fig 3. Creep-curves for different combinations of the creep-parameters.

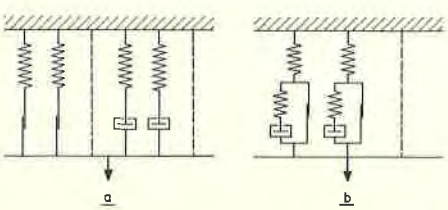

Fig 4. Models for the description of creep combined with time-independent plastic deformations.

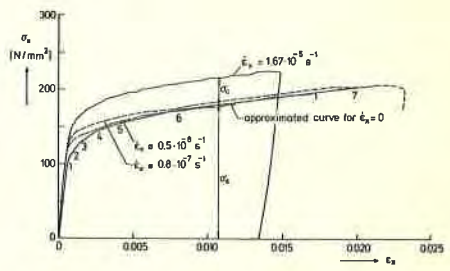

Fig 5. Strain-rate effect for WN 14948 (AISI 304)$_{2.4m}$

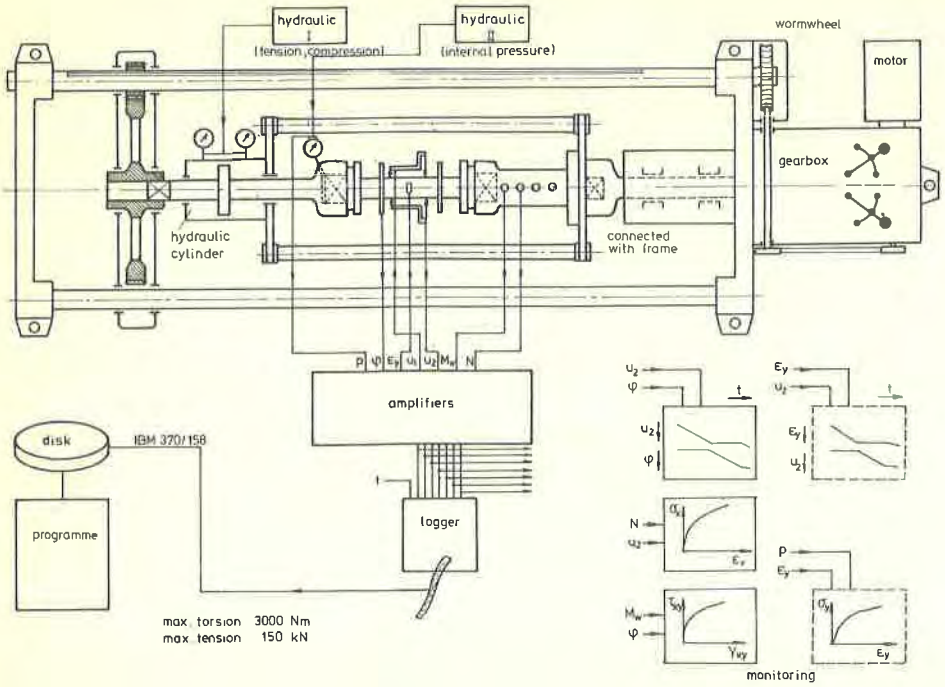

Fig 6. Tubular specimen.

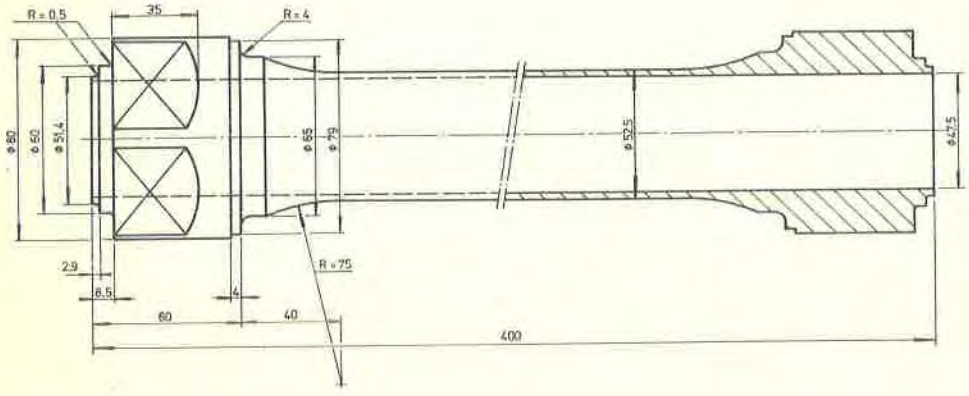

Fig 7. Test set-up.

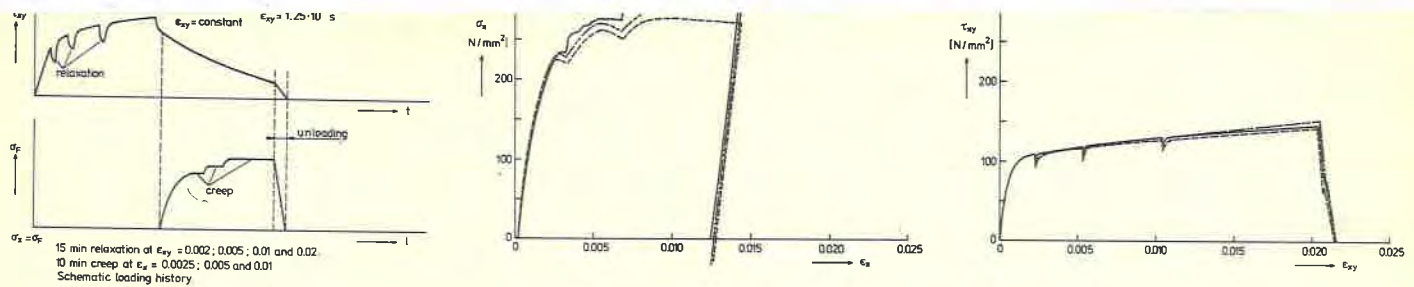

Fig 8. Torsion with relaxation periods followed by tension with creep periods ($-1 \leq \frac{\sigma_1}{\sigma_2} \leq 0$) .___ exp. results; _.._ theor. results based on tension test; _ _ _ theor. results based on torsion test.

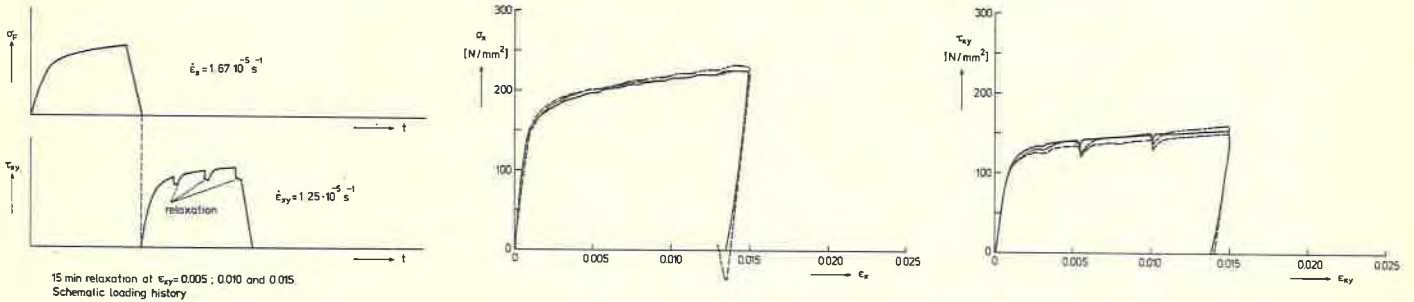

Fig 9. Tension followed by torsion with relaxation periods ($-1 \leq \frac{\sigma_1}{\sigma_2} \leq 0$).

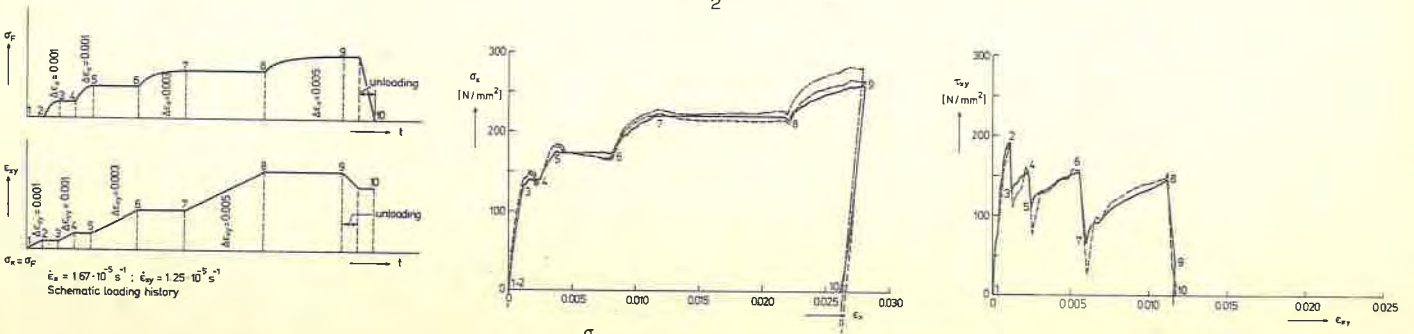

Fig 10. Loading programme in tension and torsion ($-1 \leq \frac{\sigma_1}{\sigma_2} \leq 0$).

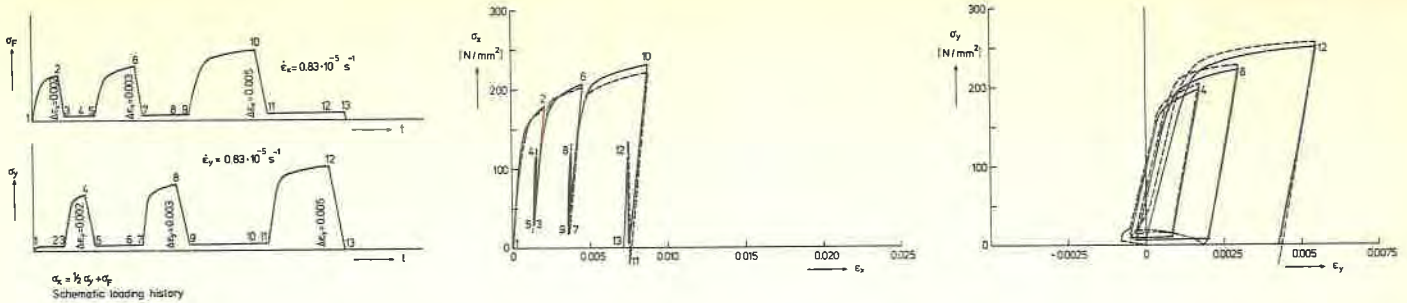

Fig 11. Loading programme in tension and internal pressure ($0 \leq \frac{\sigma_1}{\sigma_2} \leq 0.5$).

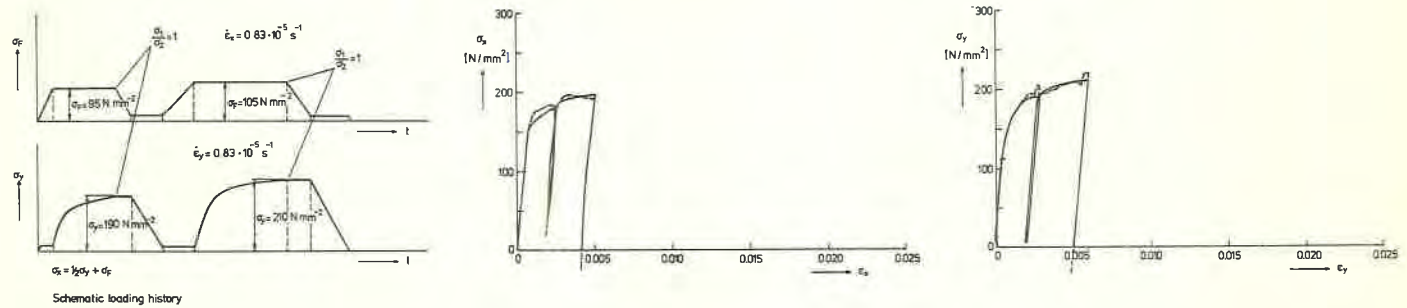

Fig 12. Loading programme in tension and internal pressure ($0 \leq \frac{\sigma_1}{\sigma_2} \leq 1$).

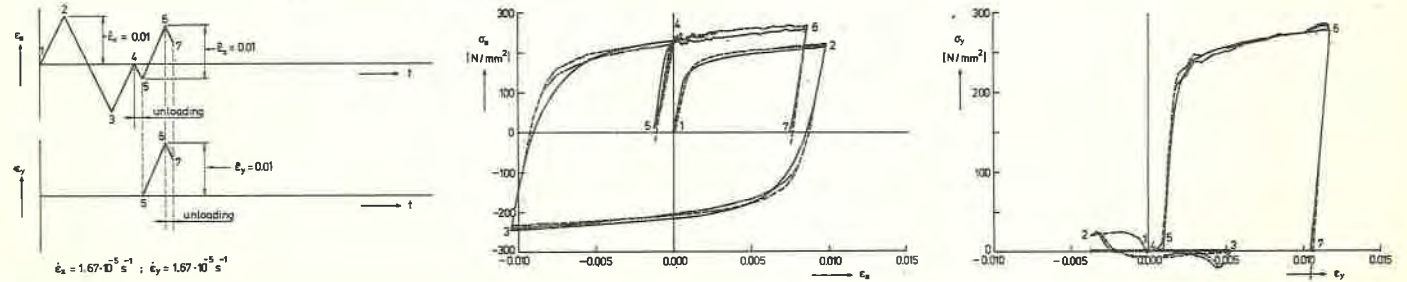

Fig 13. Axial load with loadreversal and internal pressure ($0 \leq \frac{\sigma_1}{\sigma_2} \leq 1$).